Application of coaxial superimposed hump-shaped motion planning

Wen Chen[1], Jibin Liu[2] and Jianye Wang[3,†]

[1]*Liuzhou Baosteel Automotive Steel Components Co., Ltd, Liuzhou 545001, China*
[2]*Baosteel Lasertechnik GmbH, 88212, German*
[3]*Guangdong Coordy II Laser Equipment Co., Ltd, Foshan 528300, China*
[†]*E-mail: wang__jian_ye@hotmail.com*

In this paper, in response to the demand for low cost and efficiency improvement in laser cutting, a short X-axis with high dynamic performance of small mass and short stroke superimposed on a large mass X-axis and a hump-shaped motion planning method are proposed to significantly improve the cutting efficiency. By discussing the theoretical basis of this method, it provides new ideas and ways for the development of laser cutting technology. The application of this method can bring important improvements for productivity and cost-effectiveness in the field of laser cutting, which is of great significance for industrial applications.

Keywords: Laser cutting; Coaxial superposition; Hump-shaped motion planning; Dynamic performance; Cutting efficiency.

1. Introduction

The cutting head motion system of a flat sheet laser cutting machine is one of its core components, which determines the precision, speed and efficiency of cutting [1]. When cutting sheet metal, the laser cutting head moves rapidly in the X and Y axes to cut complex shapes according to the path set by the programmer. In the cutting process of wide panel stock, the use of gantry type X-axis motion mechanism has obvious advantages [2]. Firstly, the design of the gantry structure gives the cutting head better stability in the X-axis. Since the cutting head is suspended on the beam, it can effectively disperse the vibration generated during the cutting process and reduce the cutting error. Secondly, it can improve the rigidity of the system. The gantry structure is usually made of thick material with high rigidity, which can withstand larger cutting force and adapt to the cutting needs of wide panel materials. In the motion system of the robotic arm conveyor mechanism, the multi-axis superimposed doubled motion structure is also used [3]. For three-dimensional five-axis or flat panel laser cutting machine generally adopts the gantry machine structure, the gantry along the X-axis movement [4]. In order to ensure the rigidity of the structure, the mass of the gantry is usually close to 200 Kg. The impact and inertia forces brought by the large mass of the gantry become the bottleneck of the laser cutting machine to improve the motion performance. The improvement of motion performance means the improvement of cutting efficiency. Adding a set of short X-axis (See Figure 1) with small mass and small stroke on the gantry, short axis for short, is an effective way to improve the motion performance at low cost. This improvement is not only applicable to single-head cutting machines, but also to the kinematic structure of multi-beam (gantry) and one-beam multi-

Y. Zhang and M. Ma (eds.), *Proceedings of the 7th International Conference on Advanced High Strength Steel and Press Hardening (ICHSU 2024)*, Atlantis Highlights in Materials Science and Technology 3,
https://doi.org/10.2991/978-94-6463-581-2_81

head cutting machines [5]. Especially for one-beam-multi-head machines, the increase of short axes makes the adaptability and cutting capacity of the machine significantly improved. In this paper, by studying a typical section of linear displacement, the improvement of motion performance and cutting efficiency can be achieved by using hump-shaped motion planning.

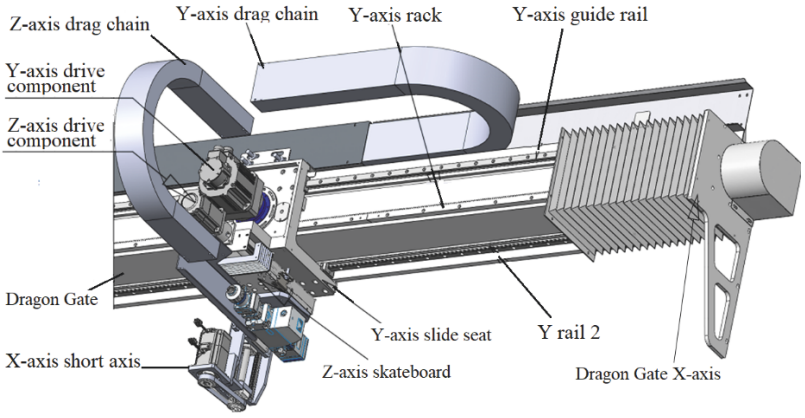

Fig. 1. The X-axis and short axis structure of the gantry beam of the laser cutting machine.

2. Boundary conditions

Let the mass of the gantry shaft be M_G and the mass of the short shaft be M_S, and it is clear that the relationship between the two is as follows:

$$M_G \gg M_S \tag{1}$$

As shown in Figure 2, the motion variables are defined as follows by the pass design of the laser cutting machine and its acceleration, acceleration, velocity, coordinate and displacement of the gantry axis are: j_G, a_G, v_G, x_G and s_G.

The acceleration, velocity, coordinates, and displacement of the short axis are j_s, a_s, v_s, x_s和 s_s, respectively. The short axis motion variables are all relative to the gantry.

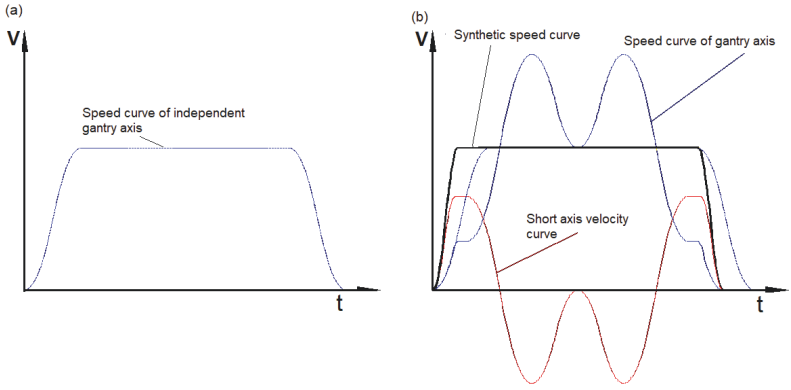

Fig. 2 (a) Independent x-axis velocity and (b) synthesized velocity curve

The permitted acceleration, permitted acceleration and permitted speed of the gantry are: : J_{GMax}, A_{GMax} and V_{GMax}, The permitted acceleration, permitted acceleration and permitted velocity of the short X-axis are: J_{SMax}、A_{SMax} and V_{SMax}.

From this we can see,

$$\begin{cases} J_{SMax} > J_{GMax} > 0 \\ A_{SMax} > A_{GMax} > 0 \\ V_{SMax} > V_{GMax} > 0 \end{cases} \tag{2}$$

The travel of the short axis on the gantry axis is 2Ss and the origin is in the center, so the coordinates of the short axis x_S should satisfy.

$$-S_S \le x_S \le S_S \tag{3}$$

3. Velocity analysis of the independent motion of the gantry

The gantry moves from the origin of X-axis to the positive direction for a certain distance and stops in a stationary state, and its motion process can be divided into seven stages of acceleration [0, T_{G1}), uniform acceleration [T_{G1}, T_{G2}), deceleration [T_{G2}, T_{G3}), uniform velocity [T_{G3}, T_{G4}), deceleration [T_{G4}, T_{G5}), uniform deceleration [T_{G5}, T_{G6}), and acceleration and deceleration [T_{G6}, T_{G7}], as shown in Figure 3 shown. Where [0, T_{G3}) are collectively referred to as the acceleration section and [T_{G4}, T_{G7}] are collectively referred to as the deceleration end. The uniform velocity section moves at the operating speed v_W.

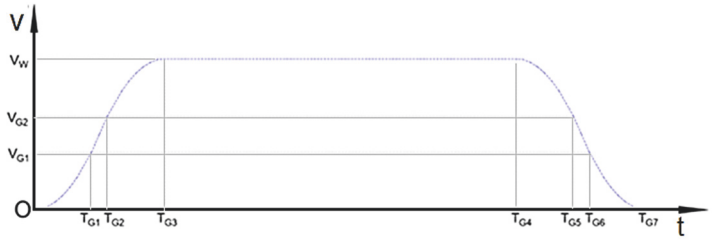

Fig. 3 Velocity-time curve of the gantry independent motion

The velocity curves for acceleration, deceleration, deceleration and acceleration and deceleration are all 2 times curves and the rest are straight lines. The velocity equation for the process of motion is,

$$v_G(t) = \begin{cases} \frac{1}{2}J_{GMAX}t^2 & 0 \le t < T_{G1} \\ v_{G1} + A_{GMAX}(t - T_{G1}) & T_{G1} \le t < T_{G2} \\ v_W - \frac{1}{2}J_{GMAX}(t - T_{G3})^2 & T_{G2} \le t < T_{G3} \\ v_W & T_{G3} \le t < T_{G4} \\ v_W - \frac{1}{2}J_{GMAX}(t - T_{G4})^2 & T_{G4} \le t < T_{G5} \\ v_{G2} - A_{GMAX}(t - T_{G5}) & T_{G5} \le t < T_{G6} \\ v_{G1} - \frac{1}{2}J_{GMAX}(t - T_{G6})^2 & T_{G6} \le t < T_{G7} \end{cases} \tag{4}$$

Among them,

$$T_{G1} = \frac{A_{GMAX}}{J_{GMAX}}$$

$$v_{G1} = \frac{1}{2}J_{GMAX}T_{G1}{}^2$$
$$v_{G2} = v_{G1} + A_{GMAX}(T_{G2} - T_{G1}) = v_W - \frac{1}{2}J_{GMAX}(T_{G3} - T_{G2})^2$$
$$T_{G7} - T_{G4} = T_{G3}$$
$$T_{G7} - T_{G5} = T_{G2}$$
$$T_{G7} - T_{G6} = T_{G1}$$

The gantry moves at a constant speed during the period $T_{G3} \le t < T_{G4}$. As it will be shown later, after the coaxial superposition of the hump-shaped motion planning, the degree of efficiency enhancement is independent of the motion in the uniform velocity section. Meanwhile, since the acceleration and deceleration segments are symmetrical, it is sufficient to examine only the acceleration segment.

4. Coaxial superimposed hump-shaped motion planning

The coaxial superimposed motion uses a hump-shaped velocity planning method, which is a computationally small, versatile and effective method.

4.1. *Movement processes*

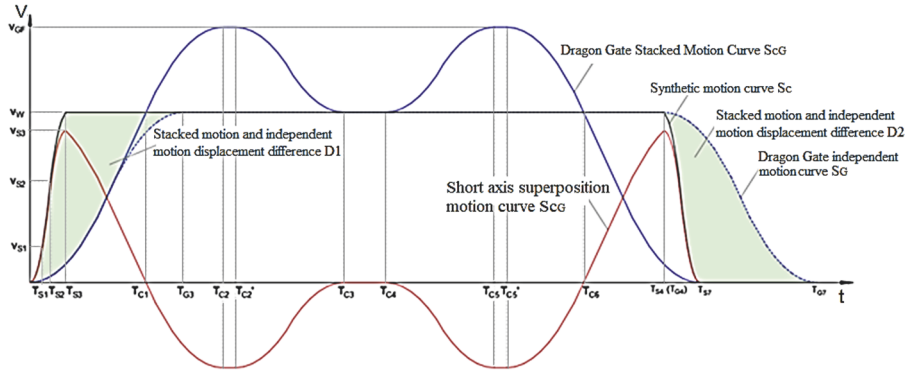

Fig.4. Velocity-time curve of the hump superposition motion

Starting the motion from rest, both the gantry axis and the short axis start accelerating at maximum capacity, as shown in Figure 4. The synthetic velocities during the motion are as follows.

$$v(t) = v_g(t) + v_s(t) \tag{5}$$

Due to the high motion performance of the short axis, the speed of the synthesized motion rapidly increases. At t=T_{S3}, the synthesized speed reaches v_W, and the short axis begins to follow the gantry axis for compensating motion, maintaining the working speed v_W. At this time, the gantry axis continues to accelerate while the short axis decelerates. From (2), it can be seen that the motion switching at time T_{S3} is easily achieved using numerical algorithms.

When $t = T_{C1}$, the gantry axis continues to accelerate, and the short axis begins to turn around and move in the negative direction.

When $t = T_{C2}$, the motion speed of the gantry axis reaches v_{GF}, where, $v_{GF} \leq V_{GMax}$ and then begins a small segment of uniform motion. The short axis also begins a small segment of uniform motion. This small segment of uniform motion between the gantry axis and the short axis is called the reset adjustment motion.

4.2. *Short axis origin and reset*

The purpose of designing a camel hump shaped speed time curve is to ensure that the short axis can return to the origin in a timely manner while leading the acceleration and deceleration of the cutting motion, that is, the short axis can be reset. The stroke of the short axis is very short, and timely resetting is necessary to play a dominant role in acceleration and deceleration in each movement, as shown in Figure 5.

The definition of the origin of the short axis is based on equation (3). As shown in Figure 3, the first hump is located between $0 \leq t < T_{C3}$. The short axis starts from the origin and undergoes a positive displacement of D_3 to time T_{C1}, followed by a negative displacement of D_4 to time T_{G3} before returning to the origin. Therefore,

$$D_3 = D_4$$

During the period of $T_{C2} \leq t < T'_{C2}$, the system performs zeroing adjustment motion. Adjust the duration to,

$$T_A = T'_{C2} - T_{C2}$$

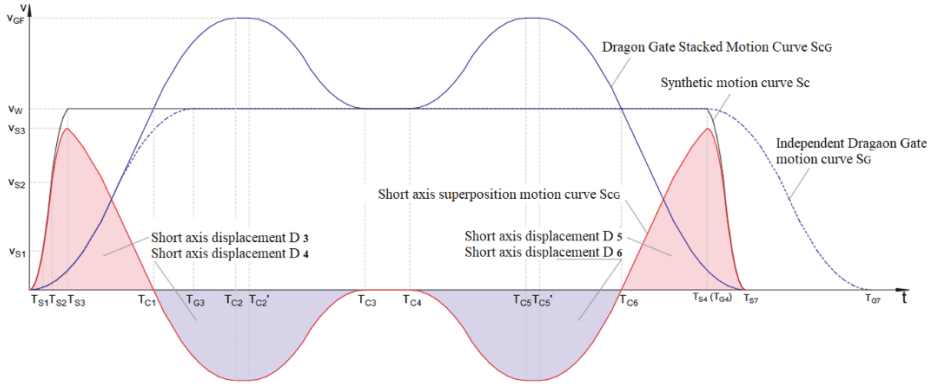

Fig. 5 Speed time curve of camel hump superposition motion

By using computer numerical analysis methods, the solution can be obtained to ensure that D_3 and D_4 are equal v_{GF}, and to adjust the duration of time, denoted as T_A.

The second hump occurs between $T_{C4} \leq t < T_{S7}$ with the short axis starting from the origin and negatively displaced by D_6 to time T_{C6} then positively displaced by D_5 to time T_{S7}, returning to the origin. Therefore,

$$D_5 = D_6$$

actually,

$$D_3 = D_4 = D_5 = D_6 \tag{6}$$

4.3. *Velocity equation of gantry axis in synthetic motion*

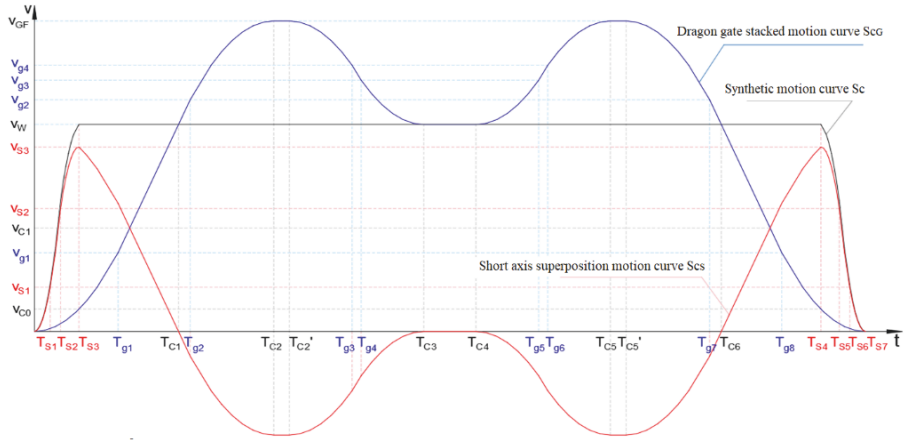

Fig.6 Speed time curve of camel hump superposition motion

As shown in Figure 6, the velocity time curve S_{CG} of the gantry in the superimposed composite motion exhibits a camel hump shape, which is mathematically expressed as,

$$v_g(t)=\begin{cases}\frac{1}{2}J_{GMAX}t^2 & 0\le t<T_{g1}\\ v_{g1}+A_{GMAX}(t-T_{g1}) & T_{g1}\le t<T_{g2}\\ v_{GF}-\frac{1}{2}J_{GMAX}(t-T_{C2})^2 & T_{g2}\le t<T_{C2}\\ v_{GF} & T_{C2}\le t<T'_{C2}\\ v_{GF}-\frac{1}{2}J_{GMAX}(t-T'_{C2})^2 & T'_{C2}\le t<T_{g3}\\ v_{g4}-A_{GMAX}(t-T_{g3}) & T_{g3}\le t<T_{g4}\\ v_{g3}-\frac{1}{2}J_{GMAX}(t-T_{g4})^2 & T_{g4}\le t<T_{C3}\\ v_W & T_{C3}\le t<T_{C4}\\ v_W+\frac{1}{2}J_{GMAX}(t-T_{C4})^2 & T_{C4}\le t<T_{g5}\\ v_{g3}+A_{GMAX}(t-T_{g5}) & T_{g5}\le t<T_{g6}\\ v_{GF}-\frac{1}{2}J_{GMAX}(t-T_{C5})^2 & T_{g6}\le t<T_{C5}\\ v_{GF} & T_{C5}\le t<T'_{C5}\\ v_{GF}-\frac{1}{2}J_{GMAX}(t-T'_{C5})^2 & T'_{C5}\le t<T_{g7}\\ v_{g2}-A_{GMAX}(t-T_{g7}) & T_{g7}\le t<T_{g8}\\ \frac{1}{2}J_{GMAX}(t-T_{S7})^2 & T_{g8}\le t<T_{S7}\end{cases} \quad (7)$$

4.4. *Velocity equation of short axis in synthetic motion*

As shown in Figure 4, the velocity time curve S_{CS} of the short axis in the superimposed synthetic motion exhibits an inverted hump shape, which is mathematically expressed as,

$$v_s(t) = \begin{cases} \frac{1}{2}J_{SMAX}t^2 & 0 \le t < T_{S1} \\ v_{S1} + A_{SMAX}(t - T_{S1}) & T_{S1} \le t < T_{S2} \\ v_{S3} - \frac{1}{2}J_{SMAX}(t - T_{S3})^2 & T_{S2} \le t < T_{S3} \\ v_W - v_g(t) & T_{S3} \le t < T_{S4} \\ v_{S3} - \frac{1}{2}J_{SMAX}(t - T_{S4})^2 & T_{S4} \le t < T_{S5} \\ v_{S2} - A_{SMAX}(t - T_{S5}) & T_{S5} \le t < T_{S6} \\ v_{S1} - \frac{1}{2}J_{SMAX}(t - T_{S6})^2 & T_{S6} \le t < T_{S7} \end{cases} \tag{8}$$

4.5. *Computer Numerical Algorithm for Coaxial Stacking Hump Motion Planning*

To achieve coaxial superimposed camel hump motion planning, it is necessary to solve the key parameters in equations (7) and (8), such as time node T_{XN}, velocity node v_{XN}, adjustment time period T_A, and velocity v_{GF}. Due to the complexity of mathematical models, it is very difficult to seek analytical solutions for these nonlinear equations. Therefore, in practical applications, computer numerical algorithms can be used to calculate, and iterative methods or heuristic search algorithms need to be used to approximate the optimal solution.

5. Conclusion

The coaxial superimposed hump-shaped motion planning method introduced in this paper represents a significant advancement in the field of laser material deposition, specifically addressing the limitations of motion performance inherent in large-mass gantry structures. By integrating a short X-axis with high dynamic capabilities onto the large mass X-axis of the gantry laser cutting machine, and employing hump-shaped motion planning, we have achieved a notable reduction in overall motion time. Empirical tests indicate a remarkable 10% enhancement in cutting efficiency, underscoring the practical benefits of this innovative approach.

This method not only optimizes overall motion time but also substantially extends the duration of homogeneous motion. The increase in homogeneous motion time plays a crucial role in enhancing the accuracy and stability of the laser cutting process, thereby improving the quality of the cuts produced. Furthermore, the implementation of a small mass, short stroke short axis system significantly boosts motion performance while maintaining a low cost, making this approach economically viable compared to the alternative of replacing the entire large mass gantry system.

In addition to its cost-effectiveness, the versatility and low computational demands of the hump-shaped velocity planning method make it an attractive option for various applications. Its minimal computational requirements facilitate easy implementation across different types of lasers cutting machines and similar industrial automation equipment, ensuring broad applicability in the field.

Moreover, the carefully engineered hump-shaped speed-time curve guarantees that the short axis can promptly return to its origin during the acceleration and deceleration phases

of the cutting movement, effectively realizing the reset of the short axis. This design ensures that the short axis maintains a leading role throughout the movement, further enhancing the overall performance of the system. Overall, the coaxial superimposed hump-shaped motion planning method offers innovative solutions for the advancement of laser material deposition technology, presenting significant industrial application value.

References

1. Lin Xiaoxia, Mo Yongkang, Yin Huaihua, Cao Xiaochen, etc. Finite Element Dynamic Analysis and Optimization of The Laser Cutting Machine Crossbeam. MECHANICAL & ELECTRICAL ENGINEERING TECHNOLOGY. 2024(7): 1-7. https://link.cnki.net/urlid/44.1522.TH.20240607.1118.004
2. J. Y. Wang, P. Zhang, Y. P. Yang, J. W. Xie. The Principle and Control Method of Belt Support Industrial Laser Cutting Machine. Proceedings of the 6th International Conference on Advanced High Strength Steel and Press Hardening (ICHSU 2022), Atlantis Press:421-426.https://doi.org/10.2991/978-94-6463-114-2_56
3. WANG Liang，ZHANG Xueqin，WANG Yilin，ZHANG Yisheng. Research and Application of Variable Speed Cooperative Transfer Control Strategy of Dual Manipulators. China Mechanical Engineering, 2020,31 (16): 1985-1990
4. Qiao, P., Tang, Q., Hu, T. et al. Post-processing technology of the five-axis additive–subtractive composite manufacturing machine tool. Int J Adv Manuf Technol 131, 409–424 (2024). https://doi.org/10.1007/s00170-024-13095-9.
5. J. Y. Wang，J. H. Zhong，G. C. Wang and L. Wang. Automatic Generation of Laser Blanking Toolpath for Multiple Cutting Heads on One Beam. Proceedings of the 5th International Conference on Advanced High Strength Steel and Press Hardening (ICHSU2020)，Inno Science Press，ISBN 978-981-5038-19-4, P.460~469.